Contact Properties of $Au/Mg_{0.27}Zn_{0.73}O$ by Different Annealing Processes

S. Han,[†,‡] J. Y. Zhang,[†] Z. Z. Zhang,*[,†] L. K. Wang,[†,‡] Y. M. Zhao,[†,‡] J. Zheng,[†,‡] J. M. Cao,[§] B. Yao,[†] D. X. Zhao,[†] and D. Z. Shen[†]

Key Laboratory of Excited State Processes, Changchun Institute of Optics, Fine Mechanics and Physics, Chinese Academy of Sciences, 3888 Dongnanhu Road, Chang Chun 130033, People's Republic of China, Graduate School of the Chinese Academy of Sciences, Beijing 100039, People's Republic of China, and Changchun University of Science and Technology, 7089 Weixing Road, Changchun130022, People's Republic of China

Received: September 15, 2010; Revised Manuscript Received: November 5, 2010

Au contacts were fabricated on $Mg_{0.27}Zn_{0.73}O$ thin films that had been annealed by different processes. For the as-grown and vacuum annealed thin films, the Au/MgZnO contacts show ohmic behavior. For the thin film annealed in vacuum followed by in air, the contact shows current−voltage curve with Schottky characteristics and ultraviolet photo response at 0 V bias. This Schottky contact is attributed to the decrease of grain boundary density during vacuum annealing and the repair of defects during succedent annealing in air. At 5 V bias, the UV/visible (330 nm/440 nm) reject ratio of the Schottky detector reaches 4 orders of magnitude, obviously higher than the non-Schottky ones based on the as-grown MgZnO thin films and the vacuum annealed ones.

Introduction

Wide bandgap semiconductors have been identified as a promising alternative in high-efficiency ultraviolet (UV) photodetectors, which could be widely used in missile warning, secure communications, flame monitoring, and so forth.[1−4] As a typical wide bandgap semiconductor, MgZnO alloys have attracted increasing interest recently. There are a few reports on wurtzite and cubic MgZnO-based photodetectors working in the region from 225 to 370 nm, which were based on metal−semiconductor−metal (MSM) structure,[5−8] Schottky structure,[9−11] even p-n junction,[12,13] and so on. Because of the easier process and higher response speed, Schottky photodiodes is a good choice before p-type doping of MgZnO is resolved. To realize a Schottky contact, a clean surface with low defect density is needed. Hydrogen peroxide pretreatment has been used to obtain Schottky contact on MgZnO.[14−16] Inevitably, this method will bring some impurities and new defects, which will results in high density trapped carriers at acceptor-like deep levels at the metal−MgZnO interface. Thermal annealing in vacuum is considered as a good way to repair some intrinsic defects in thin films. However, the escape of oxygen atoms often brings oxygen vacancies on the surface. In this paper, an $Au/Mg_{0.27}Zn_{0.73}O$ Schottky photodiode was fabricated by an annealing in vacuum followed by atmosphere. This two-step process is beneficial to both the fusion of boundary and the repair of surface states of the MgZnO film.

Experimental Methods

The MgZnO films were deposited on sapphire (0001) substrate by metal−organic chemical vapor deposition (MOCVD). The thin film thickness is about 300 nm. Dimethyl dicyclopentadienyl magnesium (MCp_2Mg), diethyl zinc (DEZn) and oxygen (O_2) with 5N purity were employed as the precursors, and nitrogen with 5N purity as the carrier gas. The deposition temperature was kept at 450 °C and the chamber pressure at 150 Torr. The flow rate of MCp_2Mg, DEZn, and O_2 were fixed at 32.8 μmol/min, 10.7 μmol/min, and 0.086 mol/min, respectively. The as-grown MgZnO thin film was cut into three pieces. One would be an evaporated Au contact without any treatment, another was annealed at 700 °C for 30 min in vacuum environment (10^{-3} Pa), and the last one was annealed at 700 °C for 30 min in vacuum environment (10^{-3}Pa) followed by annealing at 450 °C for 30 min under air environment. Thin Au contacts were made on the three MgZnO films by thermal evaporation. To examine if the Au contacts possess Schottky character, indium was used as the ohmic contact electrode.

The composition of the as-grown and annealed MgZnO thin films is measured by energy-dispersive X-ray spectroscopy (EDS) on a Hitachi S4800 scanning electron microscope (SEM). The surface morphology was also examined. The structure of the $Mg_xZn_{1-x}O$ thin films was evaluated by an X-ray diffraction (XRD) with Cu Kα (0.154 nm) line as the radiation source. The PL spectra were measured on a JY630 spectrometer with a 30 mW HeCd laser operating at 325 nm as the excitation source. The spectral response of the photodetector was measured using a 150 W Xe lamp, monochromator, chopper (EG&G 192), and lock-in amplifier (EG&G 124A). The current−voltage ($I-V$) characteristic of MSM MgZnO-based photodetector was measured by a semiconductor parameter analyzer (B1500A).

Results and Discussion

Figure 1 shows a schematic illustration of the MgZnO detectors. The thickness of three MgZnO thin films are 700 nm (as-grown), 500 nm (vacuum annealed), and 500 nm (vacuum followed by atmospheric annealed), respectively. It is said that vacuum annealing results in a decrease of the thin film components. The EDS analysis indicates that the Mg content in the three MgZnO films are 20% (as-grown), 27% (vacuum annealed), and 27% (vacuum and atmospheric annealed). It means that more Zn content in thin film escaped away than Mg content during vacuum annealing, which was attributed to the

* To whom correspondence should be addressed.
† Chinese Academy of Sciences.
‡ Graduate School of the Chinese Academy of Sciences.
§ Changchun University of Science and Technology.

10.1021/jp108795u
Published on Web 11/22/2010

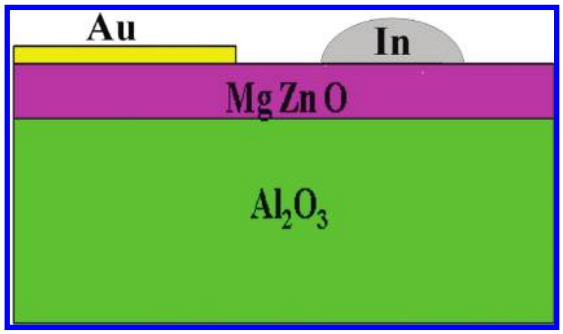

Figure 1. Schematic illustration of the MS structure MgZnO detectors.

larger vapor pressure of Zn than Mg content. The Au contact is 20 nm in thickness. Indium ohmic contact was fabricated by sintering method at 10^{-3} Pa. The space between Au and In electrodes is 1 mm. The dark $I-V$ characteristics of the detectors based on the three MgZnO films are illustrated in Figure 2a. Although gold is regarded as a good Schottky contact material, the $I-V$ curves of the contacts on the as-grown and vacuum-annealed (700 °C) MgZnO samples show ohmic characteristic. The only difference is that the dark current of vacuum annealed sample is about 70 times larger than that of the as-grown one. The low resistance may be caused by fusion together of grains, increase of donorlike defects and increase of effective contact area. For the vacuum-atmospheric annealed MgZnO film, the Au/MgZnO/In device shows a clear rectifying effect. For forward bias and $V > 3kT/q$, the $I-V$ characteristics of the Schottky diode is described by following equation according to the thermionic emission theory

$$I = A^*T^2 \exp(-q\phi_b/kT)\exp[q(V - IR_S)/nkT] \quad (1)$$

where k is Boltzmann's constant, T is absolute temperature, R_S is the series resistance, n is the ideality factor, A^* is effective Richardson coefficient and ϕ_b is barrier height. Furthermore, we can obtain the following equation from eq 1

$$\frac{dV}{d(\ln J)} = JSR + \frac{n}{\beta} \quad (2)$$

where $\beta = q/kT$, and S is the contact area. Thus, the plot of $dV/d(\ln J)$ versus J will give a straight line with slope SR, as shown in Figure 3a. and the y-axis intercept n/β. Hence the ideality factor n was determined to be 4.56.[17]

To calculate the ϕ_b, we then defined a function $H(J)$ from eq 1 as follows

$$H(J) = JSR + n\phi_b$$

where

$$H(J) = V - \frac{n}{\beta}\ln\left(\frac{J}{A^*T^2}\right) \quad (3)$$

The plot of $H(J)$ versus J will also give a straight line using the n value determined from eq 2, while the y-axis intercept is equal to ϕ_b. It can be found that the intercept value was 2.19 calculated from $H(I)$ as a function of I as shown in Figure 3b. Then the Schottky barrier height between Au and $Mg_{0.27}Zn_{0.73}O$ thin film was found to be 0.48 eV. From Figure 2b, the $I-V$ curves of the In/MgZnO/In shows a straight line. So the Schottky barrier is from the contact between Au and the two-step annealed MgZnO thin film.

Figure 4a shows the 0 V bias photoresponse spectrum of the detector fabricated by the two-step-pretreatment. The responsivity maximum occurred at 330 nm and the cut off at 345 nm. The ultraviolet photoresponse at 0 V bias voltage means there is photovoltaic effect in the Au/MgZnO/In device. It also supports the Schottky barrier between Au and MgZnO film, which is in accordance with the dark $I-V$ curve in Figure 2a.

Schottky barrier brings not only 0 V bias response, but also other advantages in photoresponse. The measurements are performed at 5 V bias; for Schottky type detector, it is −5 V bias. The response curves are shown in Figure 4b. It can be seen that the two-step-pretreated detector possesses a much sharper cutoff edge than the other two. The UV/visible rejection ratio (320 nm/440 nm) of the two-step-pretreated detector is 4 orders of magnitude, obviously higher than the other two. For photoconductive detectors without Schottky barrier, the total photocurrent of electrons and holes is

$$I_{ph} = \frac{wtq(n\mu_e + p\mu_h)V_b}{l} \quad (4)$$

where $\mu_e$is the electron mobility, $\mu_h$is the hole mobility, V_b is the bias voltage and

$$n = n_0 + \Delta n,\ p = p_0 + \Delta p \quad (5)$$

The terms n_0 and p_0 are the average thermal equilibrium carrier densities, and Δn and Δp are the photogenerated carrier concentrations. When visible light was irradiated on the detector, photogenerated carriers would be collected easily, so visible response of the detector seems high relatively, as shown in Figure 4b. For the irradiated light with energy smaller than the band gap of the MgZnO thin film, when the wavelength of the irradiated light turned shorter the number of the photogenerate carriers increased, but because the photocurrent changed linearly with photogenerate carriers, it increased less. And because the light responsivity of the detector is proportional to photocurrent, it also increased less with shorter wavelength irradiated light, and the peak responsivity value of the detector is not big. So for photoconductive detectors on grown and vacuum annealed MgZnO, the ultraviolet response spectrum of the detector is gently and the UV/visible rejection ratio of the devices is low. But for Schottky barrier detector, from the thermionic emission theory the current is

$$I_{Mst} = I_{st}\left[\exp\left(\frac{qV}{\beta kT}\right) - 1\right] \quad (6)$$

where saturation current density

$$I_{st} = A^*T^2 \exp\left(-\frac{\phi_b}{kT}\right) \quad (7)$$

where A^* is the Richardson constant, and β is an empirical constant close to unity. When negative bias voltage was added, both the negative bias voltage and schottky barrier contributed to the internal field of the detector. Because the number of

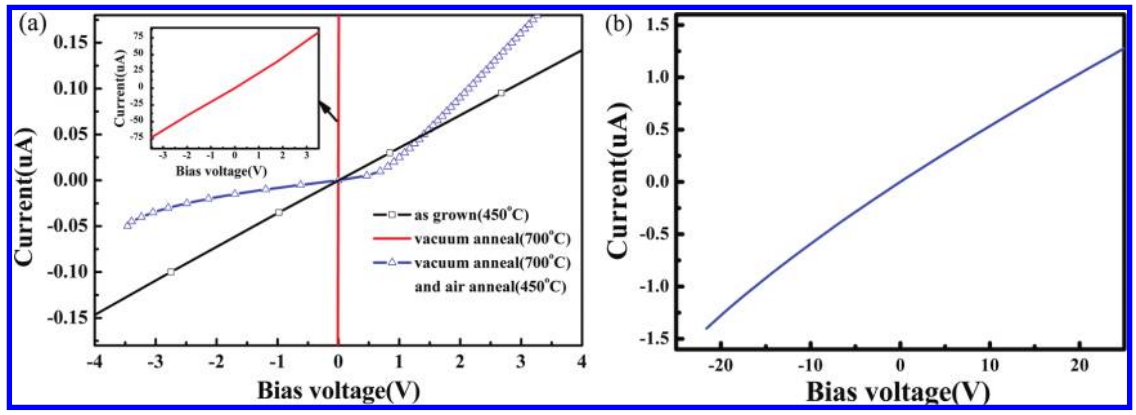

Figure 2. (a) The current−voltage ($I-V$) curves of the three detectors. (b) The current−voltage ($I-V$) curves of In/MgZnO/In for the vacuum-atmospheric annealed MgZnO thin film.

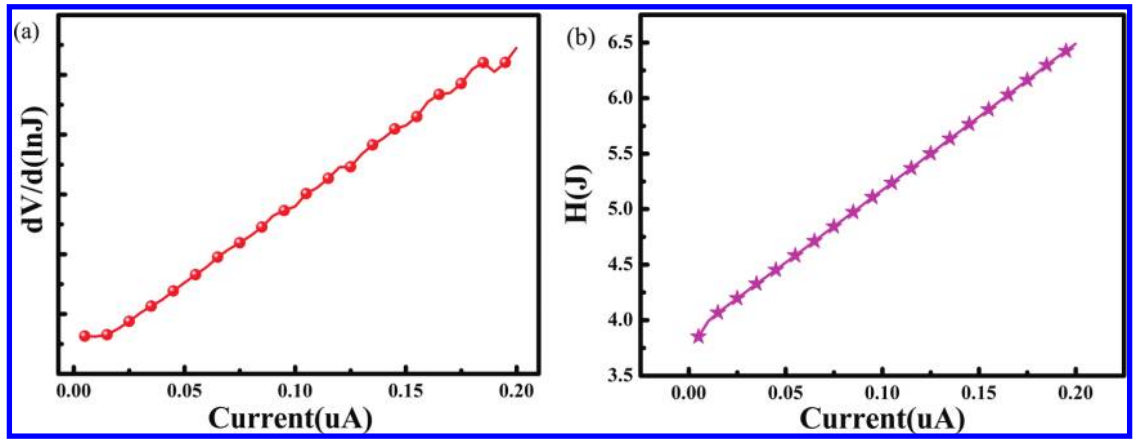

Figure 3. (a) The plot of dV/d(ln J) versus J. (b) plot of $H(I)$ as a function of I.

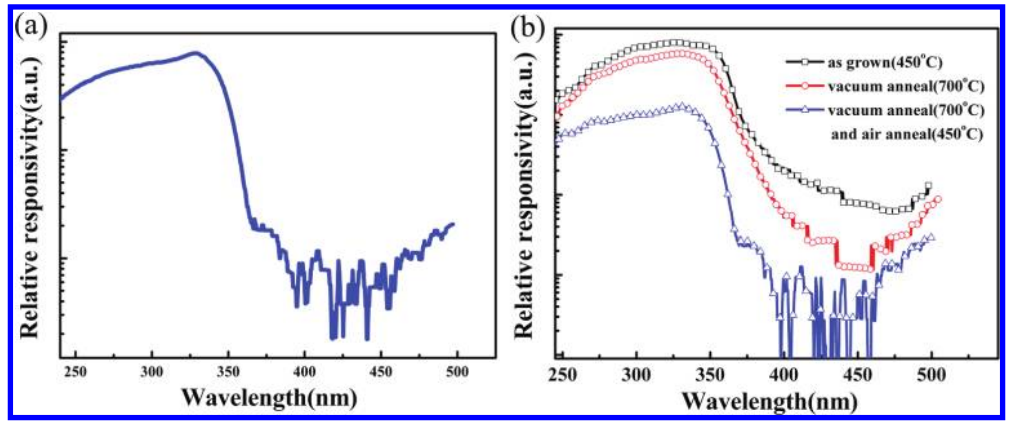

Figure 4. (a) Photoresponse spectrum of the Schottky type MgZnO detector under 0 V bias. (b) Response spectra of three detectors on as-grown and annealed MgZnO films at 5 V bias.

photogenerated carriers caused by visible light was small, its collection was blocked by the internal field, so the visible response is low. But when ultraviolet light is irradiated on the detector, because the absorption coefficient of the detector is much larger, there are large quantities of photogenerated carriers in the junction of the detector. The function of the photogenerated carriers is equal to adding a plus voltage ΔV to the junction, so the bias voltage increased to $V + \Delta V$, and the current of the detector is much higher from eq 6. Therefore, the ultraviolet response of the detector is much higher compared with visible response. Because the growth of photocurrent with bias voltage is exponential for the irradiated light with energy smaller than band gap of the MgZnO thin film, when the wavelength turned shorter the photocurrent of the detector increased much more than the photoconductive detector. Thus, the responsivity value of the detector also increased more, and this causes the sharper ultraviolet response spectrum and the high UV/visible rejection ratio of the device with Schottky junction.[18]

As shown, the vacuum-air annealing process results in the dramatic change in $I-V$ characteristic of the Au/$Mg_{0.27}Zn_{0.73}O$ contacts. According to metal−semiconductor contact theory, the most possible reason may be the change in surface states. To understand further the differences among the three samples, SEM and PL characterizations were performed. Figure 5 shows the SEM images of the samples surface, where panels a−c are for the as-grown, vacuum-treated and two-step-treated samples, respectively. As shown in Figure 5a, the as-grown MgZnO film

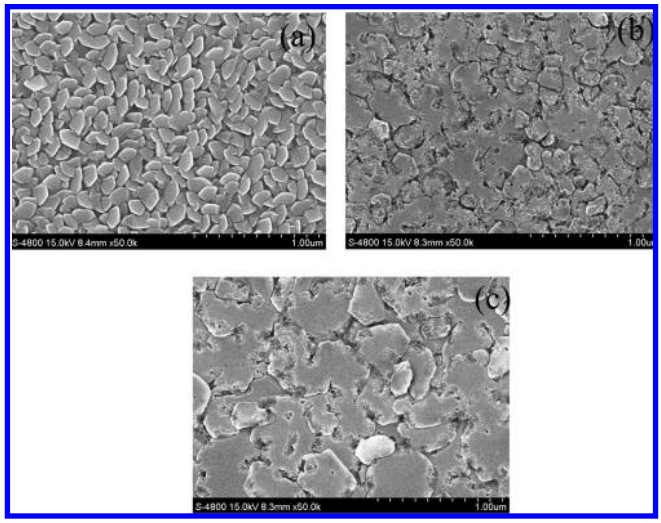

Figure 5. SEM photograph of three MgZnO thin films: (a) as-grown sample, (b) vacuum-annealed sample. (c) sample annealed in vacuum followed by air circumstance.

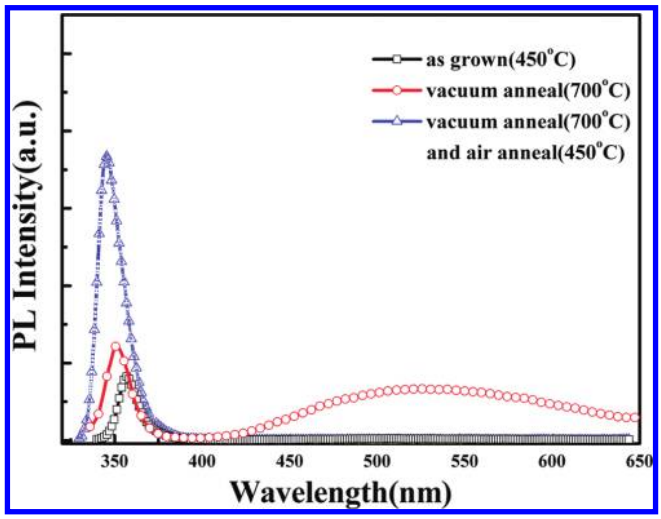

Figure 6. Room-temperature PL spectras of as-grown and annealed MgZnO thin films.

is composed of grains with uniform size of about 100 nm. It can be inferred that there are large density of defects on the grain surface and boundary due to the discontinuity of length range order. After vacuum annealing, as shown in Figure 5b, the grains tend to fuse together and the film looks smoother than the as-grown one. During the subsequent annealing in atmosphere, the grains go on to fuse each other and the surface smoothness is improved further. From the change in specific surface area, the decrease of surface defects density in vacuum should be more remarkable than the case in air subsequently. However, the $I-V$ curve does not evolve into Schottky one as expected after vacuum annealing.

Figure 6 shows the room temperature PL spectra of the as-grown and annealed MgZnO thin films. The UV PL peak shifts to large energy direction after thermal annealing, which is in accordance with the change in composition measured by EDS. In an earlier study, we also found a similar change in composition.[19] For the deep level emission band, the vacuum-treated sample shows much greater intensity than the other two. In the vacuum circumstance, the fusion among grains occurs more easily due to the absence of gas gap at the boundary. However, more oxygen atoms escape from the film than the case in atmosphere because there is no suppression by the atmosphere molecules. Therefore, the vacuum annealing often results in II-group-rich samples, as reported in ref 20. Large numbers of oxygen vacancies on the surface play deep level luminescence centers.[21,22] These oxygen vacancies on MgZnO film surface cause direct and/or trap-assisted tunneling processes at the interface between Au electrode and MgZnO. These tunneling processes result in the ohmic $I-V$ behavior of Au/MgZnO contacts[23,24] but not the Schottky ones we expect. Moreover, a large number of oxygen vacancies and the accompanying interstitial zinc decrease the film resistance significantly. It causes a large dark current, which is 400 times that of the detector on the as-grown thin film. To repair the induced defects by vacuum annealing, an appropriate annealing in circumstance-included oxygen is necessary. After a 450 °C treatment in air, the UV emission intensity shows obvious increase and the deep level PL band of the MgZnO thin film was suppressed remarkably, which means most surface states were repaired. The repair of surface state weakens the pinning effect[25] and tunneling processes. It is the main reason for the transformation from ohmic contact to Schottky contact. Because the defects repaired during air annealing are donorlike ones, the resistance of the thin film increases. The direct benefit is that the dark current of the Au/MgZnO detector decreased significantly compared with the vacuum-annealed sample.

Conclusions

A Schottky type Au/$Mg_{0.27}Zn_{0.73}O$ contact was obtained by vacuum-air pretreatment. The Au contacts on the as-grown thin film and the vacuum-annealed film show the ohmic properties. The SEM images of surface morphology indicate that vacuum annealing accelerates the fusion of the grains, which will reduce the boundary density. However, it introduces a large number of intrinsic defects, which is proven by the PL measurements. After the subsequent annealing in air at 450 °C, the intrinsic defects were found to be repaired remarkably. It is considered to be the main reason for the Schottky contact between the Au and MgZnO thin films. In conclusion, the two-step pretreatment composed of vacuum annealing and subsequent air annealing is a feasible way to improve Au/MgZnO contact properties and the photon detectors.

Acknowledgment. This work is supported by the Knowledge Innovation Program of the CAS (No. KJCX3.SYW.W01) and the National Science Foundation of China (Nos. 10974197 and 60976040).

References and Notes

(1) Zhang, D. H.; Brodie, D. E. *Thin Solid Films.* **1994**, *95*, 238.
(2) Takahashi, Y.; Kanamori, M.; Kondoh, A.; Minoura, H.; Ohya, Y. *Jpn. J. Appl. Phys.* **1994**, *33*, 6611.
(3) Studenikin, S. A.; Golego, N.; Cocivera, M. *J. Appl. Phys.* **2000**, *87*, 2413.
(4) Sharma, P.; Mansingh, A.; Sreenivas, K. *Appl. Phys. Lett.* **2002**, *80*, 553.
(5) Zhao, Y.; Zhang, J.; Jiang, D.; Shan, C.; Zhang, Z.; Yao, B.; Zhao, D.; Shen, D. *ACS Appl. Mater. Interfaces* **2009**, *1* (11), 2428–2430.
(6) Yang, W.; Hullavarad, S. S.; Nagaraj, B.; Takeuchi, I.; Sharma, R. P.; Venkatesan, T. *Appl. Phys. Lett.* **2003**, *82*, 20.
(7) Ju, Z. G.; Shan, C. X.; Jiang, D. Y.; Zhang, J. Y.; Yao, B.; Zhao, D. X.; Shen, D. Z.; Fan, X. W. *Appl. Phys. Lett.* **2008**, *93*, 173505.
(8) Du, X.; Mei, Z.; Liu, Z.; Guo, Y.; Zhang, T.; Hou, Y.; Zhang, Z.; Xue, Q.; Kuznetsov, A. Y. *Adv. Mater.* **2009**, *21*, 4625–4630.
(9) Endo, H.; Sngibuchi, M.; Takahashi, K.; Goto, S.; Sugimnra, S.; Hane, K.; Kashiwaba, Y. *Appl. Phys. Lett.* **2007**, *90*, 121906.
(10) Endo, H.; Kikuchi, M.; Ashioi, M.; Kashiwaba, Y.; Hane, K.; Kashiwaba, Y. *Appl. Phys. Express* **2008**, *1*, 0512011.
(11) Jiang, D. Y.; Shan, C. X.; Zhang, J. Y.; Lu, Y. M.; Yao, B.; Zhao, D. X.; Zhang, Z. Z.; Fan, X. W.; Shen, D. Z. *Cryst. Growth Des.* **2009**, *9*, 454–456.

(12) Liu, K. W.; Shen, D. Z.; Shan, C. X.; Zhang, J. Y.; Yao, B.; Zhao, D. X.; Lu, Y. M.; Fan, X. W. *Appl. Phys. Lett.* **2007**, *91*, 201106.
(13) Ohta, H.; Hirano, M.; Nakahara, K.; Maruta, H.; Tanable, T.; Kamiya, M.; Kamiya, T.; Hosono, H. *Appl. Phys. Lett.* **2003**, *83*, 1029.
(14) Gu, Q. L.; Cheung, C. K.; Ling, C. C.; Ng, A. M. C.; Djurišić, A. B.; Lu, L. W.; Chen, X. D.; Fung, S.; Beling, C. D.; Ong, H. C. *J. Appl. Phys.* **2008**, *103*, 093706.
(15) Kim, S.-H.; Kim, H.-K.; Seong, T.-Y. *Appl. Phys. Lett.* **2005**, *86*, 112101.
(16) Tabares, G.; Hierro, A.; Ulloa, J. M.; Guzman, A.; Muñoz, E.; Nakamura, A.; Hayashi, T.; Temmyo, J. *Appl. Phys. Lett.* **2010**, *96*, 101112.
(17) Cheung, S. K.; Cheung, N. W. *Appl. Phys. Lett.* **1986**, *49*, 85.
(18) Razeghi, M.; Rogalski, A. *J. Appl. Phys.* **1996**, *79* (10), 15.
(19) Han, S.; Shen, D. Z.; Zhang, J. Y.; Zhao, Y. M.; Jiang, D. Y.; Ju, Z. G.; Zhao, D. X.; Yao, B. *Vacuum* **2010**, *84*, 1149–1153.
(20) Kim, Y. Y.; An, C. H.; Cho, H. K.; Kim, J. H.; Lee, H. S.; Jung, E. S.; Kim, H. S. *Thin Solid Films.* **2008**, *516*, 5602–5606.
(21) Wu, X. L.; Siu, G. G.; Fu, C. L.; Ong, H. C. *Appl. Phys. Lett.* **2001**, *78*, 2285.
(22) Liu, X.; Wu, X.; Cao, H.; Chang, R. P. H. *J. Appl. Phys.* **2004**, *95*, 3141.
(23) Brillson, L. J.; Mosbacker, H. L.; Hetzer, M. J.; Strzhemechny, Y.; Jessen, G. H.; Look, D. C.; Cantwell, G.; Zhang, J.; Song, J. J. *Appl. Phys. Lett.* **2007**, *90*, 102116.
(24) Mosbacker, H. L.; Strzhemechny, Y. M.; White, B. D.; Smith, P. E.; Look, D. C.; Reynolds, D. C.; Litton, C. W.; Brillson, L. J. *Appl. Phys. Lett.* **2005**, *87*, 012102.
(25) Allen, M. W.; Durbin, S. M. *Appl. Phys. Lett.* **2008**, *92*, 122110.

JP108795U